PERFORMANCE OF TRANSMULTIPLEXERS BASED ON OVERSAMPLED FILTER BANKS UNDER VARIABLE OVERSAMPLING RATIOS

Stephan Weiss, Andrew P. Millar, Robert W. Stewart and Malcolm D. Macleod

Department of Electronic and Electrical Engineering
University of Strathclyde, Glasgow G1 1XW, Scotland, UK
{stephan.weiss,andrew.millar,r.stewart}@eee.strath.ac.uk

ABSTRACT

In this paper, we explore the influence of oversampling on a filter bank based transmultiplexer, for which previous research has established oversampling as a useful mean to ease synchronisation. The effect of oversampling is assessed mainly in terms of inter-symbol interference due to synchronisation errors and due to the residual time-dispersive effect of the transmission medium after transmultiplexing. Both effects can be targetted by a fractionally spaced equaliser. Although the achievable minimum mean square error is lower for higher oversampling ratios, we show by example of a powerline communications channel that slow convergence of least mean square type adaptive equalisers prohibits the exploitation of this benefit. Together with considerations on bandwidth efficiency and peak-to-average power ratio, it is advantageous to keep the oversampling ratio as small as possible.

1. INTRODUCTION

Transmultiplexing using filter banks is one of the oldest multiplexing methods in telecommunications [1, 2]. While the design of critically sampled structures, which are free of redundancy, was a break-through in terms of signal processing theory [3, 4], these systems lose their orthogonality when communicating over dispersive channels. This has been remedied by means of equalisation, which however requires cross-terms between subbands [5] — equivalent to [6] for the dual operation of signal decomposition — or other forms of interference mitigation, see e.g. [7], in order to achieve a meaningful system performance.

Some of the problems encountered in critically sampled transmultiplexers can be addressed by oversampling [8, 9], which leads to simplified transceiver structures [10]. Oversampling offers additional advantages in the presence of structured noise and interference where the low-noise subspace can be used for transmission [11, 12]. Advantages over OFDM systems in terms of redundancy and resilience to synchronisation errors have been demonstrated [10, 13, 14, 15].

Various filter bank techniques have been investigated in the past for transmultiplexing, including modified DFT (MDFT) filter banks [16], OFDM/OQAM wavelet filter banks [16, 17], cosine modulated filter banks [18], or DFT [19] or generalised DFT (GDFT) filter banks [13, 20]. Most of these transmultiplexers permit efficient implementations; in particular the GDFT approach has been demonstrated to yield a very low complexity [21, 22], that is not more costly than OFDM if channelisation filters are taken into account [13].

The oversampled transmultiplexers in [13, 21] use oversampling by a factor of two, while the oversampling ratio (OSR) — the reciprocal of a code rate — varies in different publications. Therefore the aim of this contribution is to evaluate the impact of OSR on the system performance. Some performance measures, such as the bandwidth efficiency, are clear and favour a low OSR. Others, such as the robustness to frequency offset synchronisation, have been found to prefer higher OSRs [13]. Below, we will be particularly interested in evaluating how the OSR affects the residual inter-symbol interference (ISI) in a transmultiplexer system, and the impact on fractionally spaced equalisation (FSE) in order to perform synchronisation and equalisation [5, 7]. Also, the peak-to-average power ratio (PAPR) has been investigated for filter banks compared to OFDM [23], but OSR has not been considered.

Therefore, Sec. 2 explores the transmultiplexer design and the resulting properties such as ISI and PAPR, while the FSE and its performance is highlighted in Sec. 3. Relevant simulations are included on the respective sections, and Sec. 4 provides an overall discussion and conclusions.

2. FILTER BANK BASED TRANSMULTIPLEXER

2.1 General Setup

The overall transmultiplexer system is depicted in Fig. 1, consisting of a filter bank based multiplexer in the transmitter, transmission over a dispersive channel with impulse response $c[m]$ and corrupted by additive white Gaussian noise $v[m]$, and a filter bank based demultiplexer in the receiver.

The transmitter provides a data vector $\mathbf{x}[n] \in \mathbb{C}^N$, which consists of parallel data streams that may be contributed by up to N independent users. A polyphase synthesis matrix $\mathbf{U}(z) \in \mathbb{C}^{K\times N}(z) \bullet\!\!-\!\!\circ\, \mathbf{U}[n]$ maps the data to a block of $K \geq N$ samples, which are time-multiplexed onto a signal $s[m]$, whereby the time-index m runs K times faster than n, such

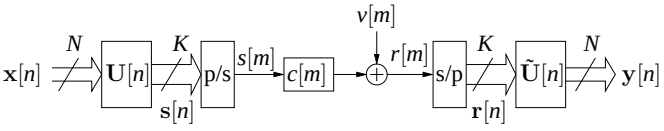

Figure 1: Overall transmultiplexer setup where a transmit vector $\mathbf{s}[n]$ is multiplexed across a noisy channel with impulse response $c[m]$, and demultiplexed into a receive data vector $\mathbf{r}[n]$ in the receiver.

 ISSN 2076-1465

that

$$\mathbf{s}[m/K] = \begin{bmatrix} s[m] \\ s[m-1] \\ \vdots \\ s[m-K+1] \end{bmatrix} \quad m = nK, n \in \mathbb{Z} \quad . \qquad (1)$$

Compared to the input data in $\mathbf{x}[n]$, the transmit signal $s[m]$ contains redundancy due to oversampling by a ratio K/N. This redundancy provides a guard band between different multiplexed frequency bands, and the variation of this OSR is the subject of this paper.

After transmission over a dispersive channel with channel impulse response $c[m]$, the signal $r[m]$ is received including additive white Gaussian noise at a specific signal to noise ratio (SNR).

At the receiver, the signal is buffered in blocks of length K and in this time-demultiplexed form passed on as a vector $\mathbf{r}[n] \in \mathbb{C}^K$ to the polyphase analysis matrix of the filter bank transmultiplexer. We here assume the use of paraunitary, i.e. perfectly reconstructing, filter banks [24], hence the analysis matrix is formed by the parahermitian $\tilde{\mathbf{U}}(z) = \mathbf{U}^{\mathrm{H}}(z^{-1}) \in \mathbb{C}^{N\times K} \bullet\!\!-\!\!\circ\, \tilde{\mathbf{U}}[n]$, providing the output vector $\mathbf{y}[n] \in \mathbb{C}^N$.

2.2 Transmultiplexer Design

The analysis and experiments in this paper are based on the equivalence between transmultiplexers and subband decompositions. We therefore use the design in [20], which was developed for near-perfectly reconstructing (NPR) oversampled GDFT modulated filter banks for subband adaptive filtering. Due to oversampling, a narrow transition band arises, which allows control of in-band aliasing and hence reduced the perfect reconstruction property to a K-band Nyquist condition [24].

Applied to transmultiplexers, the above design allocates a normalised angular bandwidth of $\frac{2\pi}{K}$ to each subchannel as passband width, and a bandwidth of $\frac{2\pi}{N}$ for the passband including the two transition bands on either side. Therefore, adjacent bands only overlap with their stopbands, thus keeping cross-talk at a level equivalent to the stopband attenuation. A number of magnitude responses $|P(e^{j\Omega})|$ for the prototype filter design are shown in Fig. 2, with parameters listed in Tab. 1. By GDFT modulation, these prototype filters can be turned into a series of bandpass filters with ascending centre frequency.

2.3 Design Parameters and Error Measures

We define two performance measures for this filter bank design — stopband energy and reconstruction error (RE). The stopband energy defines the level of inter-carrier interference (ICI),

$$\mathrm{ICI} = 10\log_{10} \int_{\pi/N}^{\pi} |P(e^{j\Omega})|^2 d\Omega \quad , \qquad (2)$$

whereby the term ICI is loosely extended to cover the interference between different subbands rather than subcarriers. Provided that measure (2) is sufficiently small, RE is the deviation of the prototype filter from a Nyquist-K or K-band filter [25] such that

N	K	L_p	OSR	ICI/[dB]	RE/[dB]
14	16	448	1.143	-53.6	-69.1
14	17	476	1.214	-62.7	-96.2
14	18	378	1.286	-64.9	-89.0
14	19	532	1.357	-103.1	-142.5
14	20	420	1.429	-98.9	-120.7
14	21	462	1.500	-116.2	-146.7
14	22	462	1.571	-132.6	-165.2
14	23	322	1.643	-89.1	-123.9
14	24	504	1.714	-142.5	-192.0
14	25	350	1.786	-113.9	-152.7
14	26	364	1.857	-125.4	-150.5
14	27	378	1.929	-112.2	-144.5
14	28	448	2.000	-150.6	-167.0

Table 1: Parameters of filter banks designed using [20].

$$\mathrm{RE} = 10\log_{10} |e^{-j\Omega\Gamma/K} - \sum_{k=0}^{K-1} P(e^{j(\Omega-2k\pi)/K})|^2 d\Omega \quad , \qquad (3)$$

where Γ is the constant group delay of the symmetric prototype lowpass filter $p[n] \circ\!\!-\!\!\bullet\, P(e^{j\Omega})$. The RE will be responsible for causing ISI even when transmitting across an ideal channel.

The filter bank design in [20] directly minimises the two error components (2) and (3), hence for a given specification, the filter bank design can produce a transmultiplexer based on a prototype filter that is just long enough to remain within the required error bounds. Performance measures for the designs utilised in this paper are listed in Tab. 1, where the prototype length L_p is constrained to integer multiples of both N and K [20], resulting in some variations of the error measures. The RE measures are under the assumption that ICI is negligible. Since RE $<$ ICI for all filter designs, in fact the reconstruction error would also be influenced — and limited — by ICI.

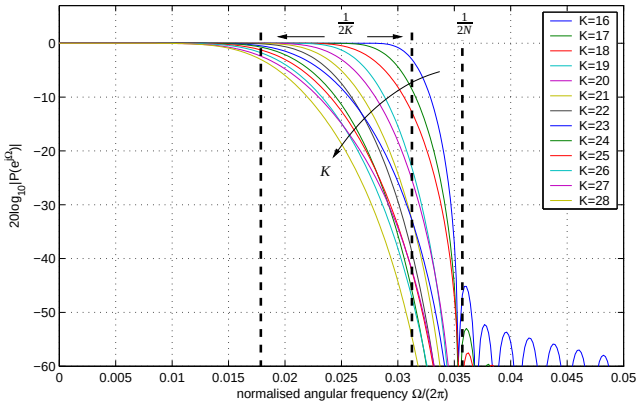

Figure 2: Magnitude responses $|P(e^{j\Omega})|$ for various prototype filters.

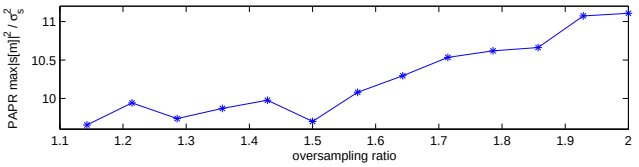

Figure 3: Peak-to-average power ratio (PAPR) for different OSRs.

2.4 Peak to Average Power Ratio

An important aspect of multicarrier systems is their often poor behaviour in terms of PAPR, which is defined as

$$\text{PAPR} = \frac{\max_m |s[m]|^2}{\sigma_s^2} \quad . \tag{4}$$

Fig. 3 provides some experimental results obtained by multiplexing 10^7 symbols onto the transmit signal $s[m]$ by using the transmultiplexers characterised in Tab. 1. As evident, there is no great impact of OSR on PAPR, except for a small rise in PAPR as the OSR is increased.

2.5 Performance Across Ideal Channel

The RE measures stated in Tab. 1 are only achievable if the receiver is perfectly synchronised with the transmitter, i.e. the Nyquist-K system between Tx and Rx is sampled at the correct time instances. In the following, we explore the transmultiplexer performance under ideal channel conditions, but with errors in timing synchronisation by introducing a variable delay $c[m] = \delta[m-\Delta]$ into the setup in Fig. 1.

If the measured impulse response for the lth channel between $\mathbf{x}[n]$ and $\mathbf{y}[n]$ is $c_l[n]$, then ISI in that channel is given by

$$\text{ISI}_l = \frac{\sum_{n=0}^{\infty} |c_l[n]|^2 - \max_n |c_l[n]|^2}{\max_n |c_l[n]|^2} \quad . \tag{5}$$

For an arbitrary subband, the ISI in dependency of the delay Δ is depicted in Fig. 4. Near-zero ISI can only be achieved at integer multiples of K from an optimal sampling point, highlighting the requirement for timing synchronisation even in the ideal channel case.

2.6 Performance Across Dispersive Channels

To test performance across a dispersive channel, a power line communications (PLC) baseband channel with 80 complex valued coefficients reported in [26] is utilised as a transmission medium. The highly dynamic magnitude response of this PLC channel is shown in Fig. 6 (top), with the characteristic of a specific transmultiplexer depicted below. The first major impact of this channel is that even though the effective channel impulse responses $c_l[n]$ are shortened by a factor of approximately K compared to $c[m]$, finite ISI will remain, because the system of filter banks and channel is no longer a Nyquist-K system.

The second impact is due to the non-constant group delay of $c[m]$, which requires timing synchronisation to be performed individually for every subband. Fig. 5 demonstrates the average ISI per subband and across all possible time delays for different OSRs. As for the ideal channel case, an increase in OSR leads to an increased robustness towards ISI.

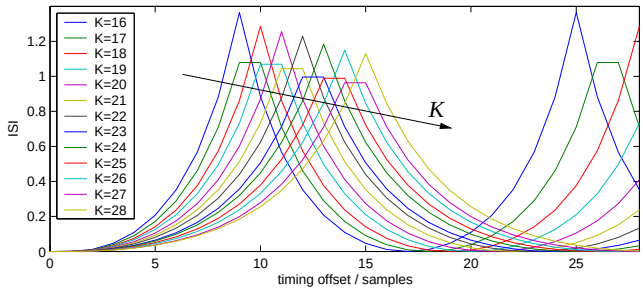

Figure 4: ISI measured in a subband for transmission over a channel $\delta[n-\Delta]$.

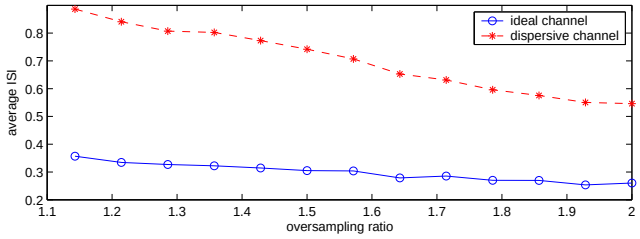

Figure 5: ISI averaged across all subbands $n = 0 \cdots (N-1)$ and all delays $\Delta \in \mathbb{Z}$, $0 \leq \Delta \leq (K-1)$ for both ideal and dispersive channels.

3. SYNCHRONISATION AND EQUALISATION

3.1 Fractionally Spaced Equaliser

In order to achieve synchronisation in individual subbands and mitigate ISI caused by a dispersive channel impulse response $c[m]$, in the following an FSE is implemented. FSEs have in the past been used for critically [7] and oversampled transmultiplexers [13]. We here utilise an FSE structure proposed in [13] which is dual to subband FSEs [27], and depicted in Fig. 7. The adaptive equaliser coefficients are contained in the diagonal polynomial matrices $\Lambda_i[n]$, where the subscript $i = \{0,1\}$ refers to the FSE's two polyphase components.

3.2 Minimum Mean Square Error Solution

Due to the separation in frequency and the negligible level of ICI afforded in the design [20], the FSEs can be designed independently in each subband. Let $c_{l,i}[n]$ be the impulse response measured between the lth component $x_l[n]$ of the transmit vector $\mathbf{x}[n]$ in Fig. 1 and the input to the lth equaliser in Λ_i in Fig. 7. Note that unlike general multirate systems, the $c_{l,i}[n]$ are linear time-invariant, thereby permitting the subsequent analysis. Defining vectors $\mathbf{c}_{l,i} \in \mathbb{C}^M$ containing the coefficients of the responses $c_{l,i}[n]$ of length M and equaliser polyphase components of length L, a convolutional matrix $\mathbf{C}_l$

$$\mathbf{C}_l = \left[\mathbf{C}_{l,0} \mid \mathbf{C}_{l,1}\right] \tag{6}$$

with the Toeplitz submatrices

$$\mathbf{C}_{l,i} = \begin{bmatrix} \mathbf{c}_{l,i} & & \mathbf{0} \\ & \mathbf{c}_{l,i} & \\ & & \ddots \\ \mathbf{0} & & \mathbf{c}_{l,i} \end{bmatrix} \in \mathbb{C}^{(L+M-1)\times L} \tag{7}$$

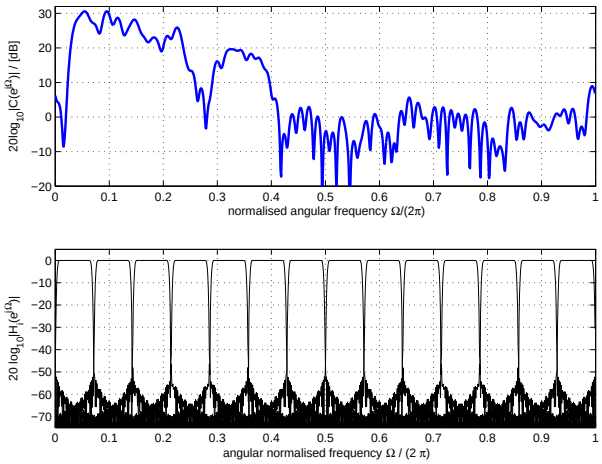

Figure 6: PLC channel magnitude response [26] (top) and transmission characteristic of transmultiplexer for $N = 14$ and $K = 16$ (bottom).

can be set up. The MMSE solution for equaliser polyphase components of length L each, organised in vectors, is given by

$$\begin{aligned} \mathbf{w}_{\mathrm{MMSE}} &= \begin{bmatrix} \underline{\lambda}_{l,0} \\ \underline{\lambda}_{l,1} \end{bmatrix} \\ &= \left(\mathbf{C}_l^{\mathrm{H}} \mathbf{R}_{x_l x_l} \mathbf{C}_l + \mathbf{R}_{v_l v_l}\right)^{-1} \mathbf{C}_l^{\mathrm{H}} \mathbf{R}_{x_l x_l} \mathbf{d} \quad . \quad (8) \end{aligned}$$

In (8), $\mathbf{R}_{x_l x_l} \in \mathbb{C}^{(L+M-1)\times(L+M-1)}$ and $\mathbf{R}_{v_l v_l} \in \mathbb{C}^{2L\times 2L}$ are the covariance matrices of the transmitted subband signal $x_l[n]$ and the channel noise measured at the equaliser input, respectively. The vector $\mathbf{d}$ is a pinning vector with zero elements except for a unit element at the Δth position, whereby Δ is the delay for the overall system.

The residual MMSE for the solution (8) is

$$\begin{aligned} \xi_{\mathrm{MMSE}} &= \mathbf{d}^{\mathrm{H}} \mathbf{R}_{x_l x_l} \mathbf{d} - \mathbf{d}^{\mathrm{H}} \mathbf{R}_{x_l x_l} \mathbf{C}_l \mathbf{w}_{\mathrm{MMSE}} \\ &\quad - \mathbf{w}_{\mathrm{MMSE}}^{\mathrm{H}} \mathbf{C}_l^{\mathrm{H}} \mathbf{R}_{x_l x_l} \mathbf{d} \\ &\quad + \mathbf{w}_{\mathrm{MMSE}}^{\mathrm{H}} \mathbf{C}_l^{\mathrm{H}} \mathbf{R}_{x_l x_l} \mathbf{C}_l \mathbf{w}_{\mathrm{MMSE}} \\ &\quad + \mathbf{w}_{\mathrm{MMSE}}^{\mathrm{H}} \mathbf{R}_{v_l v_l} \mathbf{w}_{\mathrm{MMSE}} \quad , \qquad (9) \end{aligned}$$

as shown for several different OSRs over a range of signal-to-noise ratios in Fig. 8. These results refer to the MMSE values for an FSE operating on the second subband of a transmultiplexer communicating over the PLC channel characterised in Fig. 6, with an equaliser length of $L = 30$ coefficients and a decision delay optimised with respect to the lowest achievable MMSE. Note that with an increased OSR, due to the lower ISI, the MMSE solution is considerably enhanced.

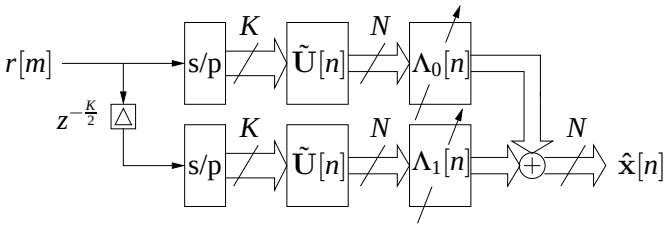

Figure 7: Receiver structure incorporating fractionally spaced equaliser.

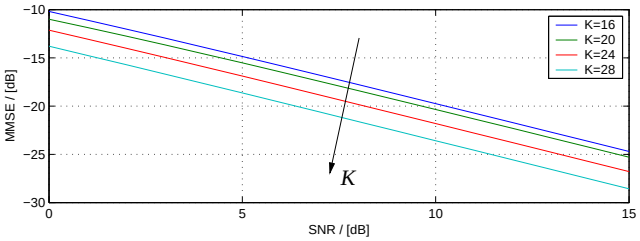

Figure 8: Residual MMSE over a range of OSRs and SNRs.

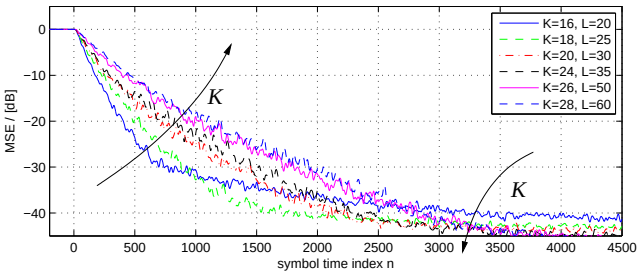

Figure 9: Convergence of FSE for transmultiplexers with different OSRs after switching on adaptation at time $n = 0$. Despite lower delay spread, the filter length L had to be increased to compensate for additional filter bank delay.

3.3 Least Mean Squares Adaptation

Various iterative adaptive algorithms can be utilised to approximate the solution in (8). We here consider LMS-type adaptation — either trained or in decision directed mode — since this class of algorithm is popular due to its low computational cost and known bounds of convergence. However, LMS-type algorithms suffer from slow convergence if the input signal is correlated, which is the case for oversampled transmultiplexers due to the bandpass characteristic of the subband signals [28]. We here use the normalised LMS (NLMS) algorithm [29] applied to the structure in Fig. 7 with the desired signal derived from the transmit signals $x_l[n]$ delayed by Δ samples.

The results for six different OSRs at an SNR of 40dB are shown in Fig. 9. In all cases, the NLMS operates with a step size of 10% of its maximum permissible value. The MMSE values for the different OSRs based on $K = \{16, 20, 28\}$ are $10\log_{10}\xi_{\mathrm{MMSE}} = \{-50, -51, -53.5\}$, respectively. Slow convergence at subband edges had previously been reported for subband adaptive filtering [28], and can also be noted here, with particularly high OSR systems converging significantly slower in the given time, even though their MMSE is lower than for low OSR systems, and they converge towards lower MSE values after a few thousand iterations.

4. DISCUSSION AND CONCLUSIONS

In this paper, filter bank based transmultiplexers operating under different oversampling ratios (OSRs) have been investigated. The transmultiplexer design is derived from a dual application for subband adaptive filtering, and the considered systems cover a range of OSRs between 1.1 and 2, with sufficiently low error measures that are directly controlled by the prototype filter design on which the utilised filter banks are based.

Since the channel impulse response experienced between the input and output of the transmultiplexer is shortened by approximately the oversampling factor, high OSRs have been shown to yield a lower level of ISI in the presence of timing synchronisation errors or a dispersive channel. Previous research in the literature has suggested fractionally spaced equalisation, which here has yielded a lower mean squared error for higher OSRs due to the reduced ISI level and shortened effective channel impulse responses. In this sense, it appears attractive to use higher OSRs, for which the filter bank design can be relaxed compared to filter banks that operate close to critical sampling.

For low OSR, the system provides less redundancy and achieves a higher spectral efficiency. Also, initial results on the peak-to-average power ratio have shown a slight advantage towards low OSRs, although more analysis and a comparison to [23] and [30] is desirable. If fractionally spaced equalisers are adapted by LMS-type algorithms, then slow convergence at the band edges can create problems. Even though systems with a high OSRs offer a lower MMSE, an LMS-type algorithm may not be able to exploit this advantage and in many cases converge significantly slower than a system operated at low OSR.

REFERENCES

[1] H. Scheuermann and H. Göckler. A comprehensive survey of digital transmultiplexing methods. *Proc. IEEE*, 69(11):1419–1450, 1981.

[2] A. Akansu, P. Duhamel, X. Lin, and M. de Courville. Orthogonal Transmultiplexers in Communication: a Review. *IEEE Trans SP*, 46(4):979–995, 1998.

[3] M. Vetterli. "Perfect Transmultiplexers". In *ICASSP*, 2567–2570, 1986.

[4] M.G. Bellanger. Specification and Design of a Prototype Filter for Filter Bank Based Multicarrier Transmission. In *ICASSP*, (4):2417–2420, 2001.

[5] T. Wiegand and N.J. Fliege. Equalizers for Transmultiplexers in Orthogonal Multiple Carrier Data Transmission. *Annals of Telecomm.*, 52(1–2):39–45, 1997.

[6] A. Gilloire and M. Vetterli. Adaptive Filtering in Subbands with Critical Sampling: Analysis, Experiments and Applications to Acoustic Echo Cancelation. *IEEE Trans SP*, SP-40(8):1862–1875, 1992.

[7] L. Vandendorpe, L. Cuvier, F. Deryck, J. Louveaux, and O. van de Wiel. Fractionally Spaced Linear and Decision-Feedback Detectors for Transmultiplexers. *IEEE Trans SP*, 46(4):996–1011, 1998.

[8] W. Kellermann. Analysis and Design of Multirate Systems for Cancellation of Acoustical Echoes. In *ICASSP*, (5):2570–2573, 1988.

[9] S. Weiss, L. Lampe, and R.W. Stewart. Efficient Subband Adaptive Filtering with Oversampled GDFT Filter Banks. In *Digest IEE Coll. Adapt. Sig. Proc. for Mobile Comm. Sys.*, 1997/383:4.1–4.9, 1997.

[10] T. Ihalainen, T.H. Stitz, M. Rinne, and M. Renfors. Channel Equalization in Filter Bank Based Multicarrier Modulation for Wireless Communications. *EURASIP J. Appl. Signal Processing*, 2007(1):140–140, 2007.

[11] F. Labeau, J.-C. Chiang, M. Kieffer, P. Duhamel, L. Vandendorpe, and B. Macq. Oversampled Filter Banks as Error Correcting Codes: Theory and Impulse Noise Correction. *IEEE TSP*, 53(12):4619–4630, 2005.

[12] S. Weiss, S. Redif, T. Cooper, C. Liu, P.D. Baxter, and J.G. McWhirter. Paraunitary Oversampled Filter Bank Design for Channel Coding. *EURASIP J. of Appl. Sig. Proc.*, 2006(1):99, 2006.

[13] A.M. Tonello and F. Pecile. A filtered multitone modulation modem for multiuser power line communications with an efficient implementation. In *ISPLC*, 155–160, 2007.

[14] A.M. Tonello, J.A. Cortes, and S. D'Alessandro. Optimal time slot design in an OFDM-TDMA system over power-line time-variant channels. In *ISPLC*, 41–46, 2009.

[15] F. Pecile and A. Tonello. On the design of filter bank systems in power line channels based on achievable rate. In *ISPLC*, 228–232, 2009.

[16] C. Siclet and P. Siohan. Weyl-Heisenberg Signal Expansions over R in $l_2(z)$ and Duality Relations Involving MDFT Filter Banks. In *ICASSP*, (6):409–12, 2003.

[17] P. Siohan, C. Siclet, and N. Lacaille. Analysis and Design of OFDM/OQAM Systems Based on Filterbank Theory. *IEEE Trans SP*, 50(5):1170–1183, 2002.

[18] P. Diniz, L. de Barcellos, and S. Netto. Design of High-Resolution Cosine-Modulated Transmultiplexers with Sharp Transition Band. *IEEE Trans SP*, 52(5):1278–1288, 2004.

[19] D. Waldhauser and J. Nossek. MMMSE Equalization for Bandwidth-Efficient Multicarrier Systems. In *IEEE Int. Symposium CAS*, 2006.

[20] M. Harteneck, S. Weiss, and R.W. Stewart. Design of Near Perfect Reconstruction Oversampled Filter Banks for Subband Adaptive Filters. *IEEE Trans CAS II*, 46(8):1081–1085, 1999.

[21] N. Moret and A. Tonello. Similarities and differences among filtered multitone modulation realization and orthogonal filter bank design. In *EUSIPCO*, 2009.

[22] S. Weiss and R. Stewart. Fast Implementation of Oversampled Modulated Filter Banks. *IEE Elect. Lett.*, 36(17):1502–1503, 2000.

[23] D. Waldhauser, L. Baltar, and J. Nossek. Comparison of Filter Bank Based Multicarrier Systems with OFDM. In *IEEE Asia Pacific Conf. CAS*, 976–979, 2006.

[24] P.P. Vaidyanathan. *Multirate Systems and Filter Banks*. Prentice Hall, 1993.

[25] R.E. Crochiere and L.R. Rabiner. *Multirate Digital Signal Processing*. Prentice Hall, 1983.

[26] S. Gault, P. Ciblat, and W. Hachem. An OFDMA based modem for powerline communications over the low voltage distribution network. In *ISPLC*, pp.42–46, 2005.

[27] H. Mohamad, S. Weiss, M. Rupp, and L. Hanzo. Fast Adaptation of Fractionally Spaced Equalisers. *IEE Elec. Lett.*, 38(2):96–98, 2002.

[28] D.R. Morgan. Slow Asymptotic Convergence of LMS Acoustic Echo Cancellers. *IEEE Trans SAP*, 2(3):126–136, 1995.

[29] S. Haykin. *Adaptive Filter Theory*. Prentice Hall, Englewood Cliffs, 2nd edition, 1991.

[30] K. Anwar, A. Priantoro, M. Saito, T. Hara, M. Okada, and H. Yamamoto. On the PAPR Reduction for Wavelet Based Transmultiplexer. In *IEEE Int. Symp. Comms. Inf. Tech.*, (2):812–815, 2004.